Unusual Size Dependence of Nonradiative Charge Recombination Rates in Acetylene-Bridged Compounds

M. Biswas,[†] Paul Nguyen,[‡] Todd B. Marder,[‡] and L. R. Khundkar*,[†]

Department of Chemistry, Northeastern University, Boston, Massachusetts 02115, and Department of Chemistry, University of Waterloo, Waterloo, ON, Canada N2L 3G1

Received: March 20, 1996; In Final Form: July 8, 1996[⊗]

Time-resolved fluorescence decays of three asymmetrically substituted phenylethynyl molecules of different size show a sizable solvent dependence. Nonradiative rate constants estimated from quantum yield and lifetime data are consistent with classical electron-transfer theory. The electronic coupling elements, H_{RP}, derived from fits of theory to the data do not follow the trend of donor−acceptor distance (or molecular size). It is found to be largest for the molecule with a butadiyne linker which is intermediate in size. Our results suggest that the bridge is directly involved in excited-state charge recombination in these conjugated molecules.

Introduction

Electron-transfer (ET) reactions have been the subject of intense scrutiny over the past several decades.[1,2] The description of rates of such reactions in terms of an electron-tunneling step driven by nuclear reorganization (solvent or intramolecular) appears to be on solid ground. More recently, researchers have begun to address the size of the electronic matrix element which describes the inherent propensity of electron transfer in proteins, DNA, and supramolecular systems. The seventies and eighties saw an explosion of activity on compounds specifically designed to test the ideas of an exponentially decaying matrix element with increasing donor−acceptor distance.[2] The idea of σ-bonds as efficient coupling links led theorists to devise ways of tracing the most efficient pathways through large macromolecules, an approach which was very successful in correlating ET rates in several modified natural proteins.[3] The general hypothesis of these studies was that the matrix element decayed exponentially with distance, distance being considered along bonds (σ, H-bonds, and short through-space jumps) and the "decay factor" being different for these three motifs.

The possible participation of "bridge-states" was highlighted by the observation that long-range ET between a donor and acceptor can be mediated by DNA if the redox species are covalently bound or intercalated to the duplex.[4] Murphy et al.[4] suggested that interactions between adjacent base pairs leads to the enhanced overlap necessary for efficient ET. Recent theoretical work using large-scale SCF calculations shows that interactions between base pairs is significant for donor−acceptor systems covalently linked to DNA.[5]

In recent years, the phenylethynyl moiety has received a great deal of attention as a building block for new (polymeric) materials, with potential applications ranging from chemical sensing to molecular electronics.[6−8] For example, they have been used to construct extended bridges (up to 16 units) and to link conjugated systems in "push−pull" devices with metalloporphyrins as chromophores.[9] Detailed knowledge of the photophysics of ethynyl (or phenylethynyl) bridged compounds is highly desirable for a better understanding of the role the bridge itself might play in photoinduced processes in such materials.

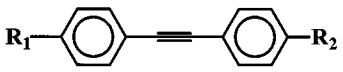

R1 = MeS; R2=CN **A**
R1 = H; R2=H **D**

R1 = MeS; R2=CN **B**
R1 = MeS; R2=MeS **E**
R1 = CN; R2=CN **F**

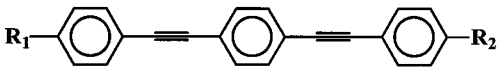

R1 = MeS; R2=CN **C**
R1 = H; R2=H **G**

Figure 1. Probe molecules **A**−**F**.

We have extended earlier studies on donor−acceptor compounds linked by a conjugated bridge[10] to systems with butadiynyl and phenylethynyl units. Here we report preliminary results on the rates of charge recombination in two new molecules, one with a butadiynyl unit and the other containing a phenylethynyl unit (Figure 1), and compare them with previous data. In all three molecules (**A**−**C**), photoexcitation induces rapid and substantial charge separation, as evidenced by the large solvatochromism observed in emission. We find that the rate of nonradiative charge recombination is larger for **B** than for the shorter diphenyl acetylene (**A**) or the longer bis(phenylethynyl) benzene (**C**). We use classical electron-transfer theory to infer that this unusual alternation in nonradiative rate constants is a consequence of electronic factors and not nuclear factors. Several possible explanations of this effect are discussed, with the conclusion that the size dependence of the matrix element is a result of direct participation of the "bridge" in the charge recombination process.

[†] Northeastern University.
[‡] University of Waterloo.
[⊗] Abstract published in *Advance ACS Abstracts,* February 15, 1997.

S1089-5639(96)00851-1 CCC: $14.00

Experimental Section

Materials and Methods of Characterization. The steady-state absorption and emission spectra (fluorescence and phosphorescence), quantum yields, and fluorescence lifetime of several compounds (Figure 1) were recorded in solvents of different polarity. The compound *p,p′*-cyanothiomethyldiphenylacetylene (**A**) was obtained as a gift from Dr. A. E. Stiegman and used to ascertain that measurements in our laboratory were consistent with previously published data.[10] The synthesis and characterization of **A** has been described previously.[11] Diphenylacetylene (tolan, **D**) was purchased from Aldrich and used as received. The compound *p,p′*-cyanothiomethyldiphenylbutadiyne (**B**), and its symmetric analogues (**E** and **F**) were synthesized in our laboratory (Northeastern University) using published procedures.[11,12] Their identity and purity was established by NMR, mass spectrometry, and HPLC. Full details will be provided elsewhere.[12] The remaining compounds **C** and **G** were synthesized and characterized at the University of Waterloo.[13,14] HPLC grade solvents were used for all reported measurements.

Optical Measurements. Steady-state absorption and emission spectra were obtained with a Perkin-Elmer Lambda 9 and a PE-LS50B, respectively. Emission spectra were not corrected for the spectral response of the instrument. Quantum yield measurements were performed on the LS50B, using quinine sulfate as a secondary standard. Several steps were taken to determine accurate quantum yields for **B**, a very weak emitter. Dilute solutions were used to avoid inner filter effects.[15] The contribution of Raman scattering from the solvent to the apparent emission spectrum was extracted by fitting the observed spectrum to a sum of several Gaussian peaks, one for each of the Raman bands and one or two for the true emission band. Only the area of the emission band was used to calculate quantum yields. The excitation energy was set to that of the first (lowest energy) discernible peak (or shoulder) in the absorption band.

The setup used to record time-resolved fluorescence decays has been described previously.[16] We obtain response functions (with 306 nm excitation) that are typically <50 ps full width at half-maximum. Fluorescence is collected with fused-silica optics and the detection wavelength selected (2 nm band-pass) using a $^1/_4$ m Heath monochromator. All measurements reported here were carried out at ambient temperature (20 ± 1 °C) in a 10 mm fused silica fluorescence cell (NSG).

Data Analysis. Each decay was fitted to a model function (sum of up to three exponentials) using the Marquardt−Levenberg nonlinear least-squares algorithm.[17] The instrument response function was accounted for in the fits by iterative reconvolution.[18] The quality of all the fits was judged to be good as shown by randomly distributed residuals and autocorrelation of weighted residuals. Typical χ^2 values ranged from 1.0 to 1.2.

Results and Discussion

Emission decays in all solvents with the exception of alcohols are predominantly single exponential. A minor ($<1\%$) decay component is sometimes observed in the decays and is most likely due to trace impurities in the sample. This is particularly noticeable in the case of **B**, which is a weak emitter.[19] The measured decays in 1-propanol and heavier alcohols are multiexponential and detection wavelength dependent. These observations are interpreted as a dynamic Stokes shift, as discussed previously for **A**.[16,20] For these solvents, we report the time constant of the major component (near the peak of the emission band) as the fluorescence lifetime. In the instances reported here, the numerical value of this time constant remains essentially unchanged across the emission band. We therefore presume that this time constant is the inverse lifetime of the equilibrated (fully solvated) state.

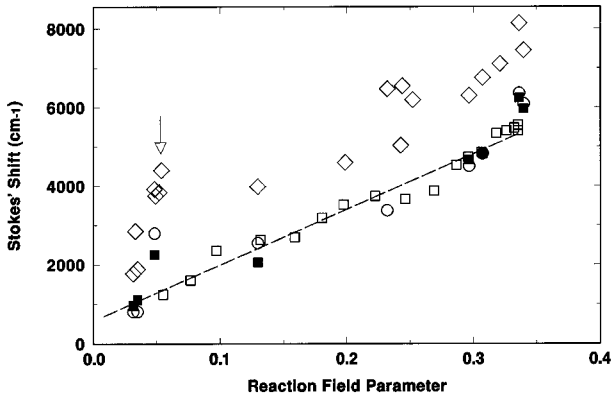

Figure 2. Solvatochromism of **A**−**C**. The open diamonds are for **A**,[10] the open circles are for **B** in different solvents, the filled boxes are for **C** in different solvents. The open boxes are for **C** in mixtures of acetonitrile and carbon tetrachloride, with the dashed line being the best fit to the Lippert equation. The arrow points at aromatic solvents which appear to result in a larger Stokes shift than predicted by the dielectric continuum model.

Absorption spectra for different probes are compared with their unsubstituted and symmetrically substituted analogues in Figure 3. The spectrum of each probe (**A**−**C**) resembles that of the related symmetric compound(s). The similarities between the different probe molecules are less striking. The spectrum of **A** (and **C**) shows broader spectral features and a red-shift compared to **D** (**G**). While the size of this shift for the **C**/**G** pair ($\simeq$2000 cm^{-1}) is consistent with a substituent effect, it is much larger for the **A**/**D** pair ($\simeq$5000 cm^{-1}), suggesting greater electronic interaction between the substituents and the diphenylethynyl moiety in the case of **A**. Likewise, a comparison of **B**, **E,** and **F** indicates that the spectrum of **B** has the same features as **E**, with a moderate red-shift. The four or five distinct peaks may be a vibronic progression in a high-frequency mode that undergoes large distortion on excitation or may correspond to one or more higher excited states.[21]

Quantum yield (QY) and lifetime data were used to determine the radiative (k_{rad}) and nonradiative (k_{nr}) rate constants using standard equations.[15,22] In each of these molecules, the quantum yield is only weakly dependent on solvent polarity. The emission lifetime of symmetric molecules (**D**−**G**) changes slightly ($<20\%$) with increasing solvent polarity, while that of asymmetric molecules (**A**−**C**) increases substantially (2−4-fold) with increasing solvent polarity. The radiative rate constant (k_r) deduced from QY and lifetime measurements are in reasonable agreement with that deduced from the integrated oscillator strength for **A** (1−3 ns), **B** (5−15 ns), and **C** (1−3 ns). The most unusual finding in our data is an alternation in the fluorescence lifetime, τ_{fl}, and consequently k_{nr}, with increasing molecular size (Table 1). In all solvents, τ_{fl} (and k_{nr}) for **B** is much smaller (larger) than in **A** or **C**. This unusual size dependence is quite intriguing. In the following sections, we discuss plausible mechanisms that could explain our observations.

Kinetic Model. In previous work on **A**, a three-state model was proposed to explain solvatochromism data and nonradiative relaxation rates in different solvents.[10] The three states considered were a polar, excited singlet, charge-transfer (^{1}CT) state, the nonpolar ground state (S_0) and a nonpolar "dark" state, which was thought to be a triplet. The dominant nonradiative channel was attributed to charge-recombination from ^{1}CT to the "dark"

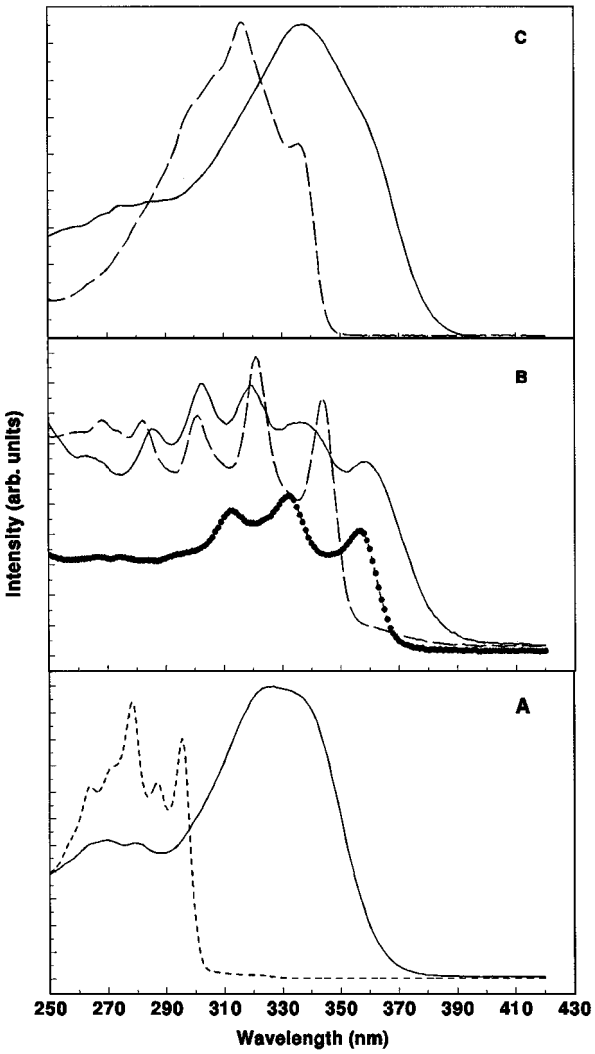

Figure 3. Absorption spectra of different molecules in methanol. Each absorption spectrum shows a small red-shift in hexane (<5 nm), with the features unchanged. (A) solid, **A**; dash, **D**; (B) solid line, **B**; circles, **E**; dash, **F**; (C) solid, **C**; dash, **G**.

state. While a fourth, locally excited state (LE) was alluded to, no direct evidence of interconversion between the LE and ^{1}CT states was found.

This model is consistent with our present measurements on **B** and **C**. In each of these molecules, the increase in the emission lifetime with increasing solvent polarity can therefore be attributed to dipolar stabilization of the emitting state. The Stokes shift is linearly dependent on the reaction field parameter (Figure 2).[24] Estimates based on the Lippert equation indicate that the dipole moment of the emitting state is quite large (>10 D). The identity of the "dark" state is yet to be unequivocally established.

Recent work has shown that the dynamics of the emitting state in **D**, which may be considered the parent molecule of **A**, is complicated by the involvement of several low-lying excited states.[25−27] In particular, there is evidence from transient absorption studies[26] that the lowest energy absorption band of **D** does not correspond to the lowest excited singlet state, S_1. The preceding discussion of the absorption spectra suggests that the spectroscopy (and dynamics) of the probe molecules may be closely related to that of the corresponding symmetric compound. Assuming that low-lying states are also present in the substituted molecules, we have expanded the kinetic model to explicitly include other relevant channels for nonradiative

TABLE 1: Spectroscopic and Lifetime Data for Probe Molecules

	quantum yield[a]			τ_{fl} (ns)		λ_{max}[c] (nm)		λ_{max}[d]
	hexane	MeCN	f[b]	hexane	MeCN	hexane	MeOH	(nm)
A	0.5	0.7	0.6	0.72	2.0	351	434	506
B	0.011	0.015	0.9[e]	0.06	0.24	374	466	534
C	0.68	0.65	0.7	0.68	1.8	376	460	551
D	0.0028[f]	0.0016[f]		0.07[g]	0.04[g]			
E	0.015	0.01		0.06	0.03	372	372	
F	0.05	0.02		0.07	0.06	376	378	
G	0.75	0.9		0.57	0.62	343	343	

[a] Measured quantum yields have an estimated random error of 15% for values greater than 0.5. The estimated random errors for **B**, **E**, and **F** are 25%. [b] The oscillator strength of the lowest energy transition (from integrated absorption) of the probe molecules in MeCN. [c] Fluorescence maximum (±1 nm) in solvents at 293 K. [d] Phosphorescence maximum (±1 nm) in methylcyclohexane at 77 K. [e] The absorption band may correspond to transitions between the ground state and more than one excited state. Thus f in this case may be overestimated. [f] Data from ref 23. [g] The lifetime of **D** appears to be excitation wavelength dependent. The numbers shown in this table were obtained using 307 nm excitation, which is on the far red-edge of the absorption band. Much smaller values (≈10 ps) are obtained with excitation at 295 nm, which is consistent with previously reported values.

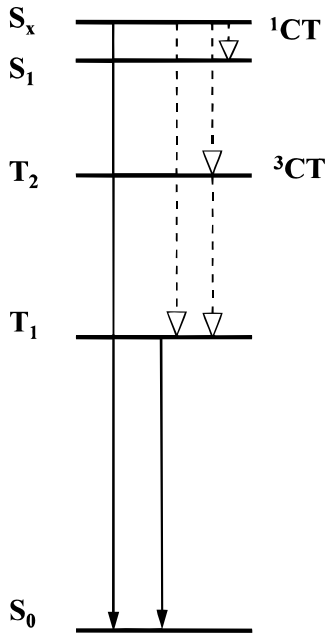

Figure 4. Kinetic scheme. The solid arrows indicate radiative processes, the dashed ones indicate nonradiative processes. See text for additional details.

decay. We designate the lowest energy transition observed in absorption in our probe molecules as one coupling S_0 to the S_x state. The nonradiative processes leading to energy relaxation from the emitting state (S_x) that we have considered are (a) S_x (^{1}CT) to S_1 (thermal charge recombination), (b) S_x (^{1}CT) to T_1 (intersystem crossing, ISC, and charge recombination to a low-lying triplet state), (c) S_x (^{1}CT) to the triplet correlated charge-transfer state (^{3}CT), and (d) other intersystem crossing processes, e.g., S_1 to T_1, the lowest energy triplet state. A kinetic scheme is shown in Figure 4. It must be emphasized that the relative ordering of S_x and S_1 may be both substituent and solvent dependent, i.e., in polar solvents, S_x has lower energy than S_1. The only radiative processes indicated in this scheme are $S_x \rightarrow S_0$ fluorescence and $T_1 \rightarrow S_0$ phosphorescence, both of which have been observed in our laboratory.

Twisted Intramolecular Charge Transfer. The kinetic scheme does not include the alternative path in which absorption creates an LE state which relaxes to the emitting CT state. In light of the growing body of results on twisted intramolecular CT (TICT) states in aromatic molecules,[28] our decision to omit this process merits some discussion. If twisting about a σ-bond were a promoting mode for CT, two internal rotations should be considered as possible candidates: (1) rotation about the phenyl acetylene σ-bond, and (2) rotation about the σ-bond between the sulfur atom and the phenyl group. Molecular mechanics[29] calculations suggest essentially free rotation about the phenyl−acetylene bond. The excitation spectrum of tolan (**D**) in a molecular beam indicates a low barrier (<200 cm^{-1}) to rotation about this bond in the ground state and probably a comparable one in the excited state.[25] The fluorescence lifetime of **D** does not show a strong solvent or viscosity dependence.[26] Ferrante et al.[30] suggested that the symmetric acetylenic stretch, rather than a low-frequency restricted torsion, is involved in coupling different electronic states. These observations argue against the involvement of twisting around the $C_6H_5-C\equiv C-$ bond in **D**, and probably in **A**. Much less is known about the characteristics of the S−phenyl bond. Molecular mechanics calculations indicate a small barrier (1.5 kcal/mol) in the ground state. No estimate is available for the barrier in excited states. However, as the thiomethyl group is common to the three probes, the dynamics of internal torsion should be similar for the molecules of interest.

Several pieces of experimental data suggest that either twisting is not important for the charge localization in the excited state of our probes or it occurs on the time scale of a few picoseconds. Changes in the shape of the emission spectrum (width and asymmetry) are smoothly correlated with solvent polarity, and the fluorescence Stokes shift increases linearly with the reaction field parameter in solvents ranging from alkanes to acetonitrile (Figure 2). Given our time resolution of $\approx$20 ps, the buildup of CT emission appears instantaneous in polar solvents that are known to have rapid solvent relaxation times.[16,31] We therefore claim that the dynamics we observe can be attributed to the ^{1}CT state. For the sake of simplicity, we have not explicitly identified the LE state in Figure 4. We treat S_x and ^{1}CT as the same electronic state (one with significant charge-transfer character) in the discussion below. It should be noted that this simplification and our use of standard expressions for estimating radiative and nonradiative rates from emission lifetimes and quantum yields assumes that if an LE $\rightarrow$ CT step is involved, the quantum yield of the ^{1}CT (S_x) state is unity.

Contribution of Multiple Low-Lying Excited Electronic States to Observed Nonradiative Decay Rates. We have measured quantum yields (Q) $\approx$ 0.8 for **A** and **C**. This implies that other nonradiative processes contribute minimally to energy relaxation and the observed dynamics. In these systems, we would not be in great error by attributing the nonradiative process entirely to charge recombination. On the other hand, the Q of **B** is small in all solvents. It is therefore important to consider the contribution of additional nonradiative channels to relaxation.

There has been recent discussion in the literature regarding the proper relative ordering of the electronic states in diphenylacetylene (tolan) and its monosubstituted derivatives. Since our probe molecules can be considered to be derivatives of or closely related to tolans, we present a brief summary of the results of Hirata et al.[27] Tolan is believed to have D_{2h} symmetry in both the ground and excited states. There has been some debate regarding the relative ordering of a B_{1u} (one-photon allowed) state and a A_{1g} (two-photon allowed) state.[25,26,32] Hirata et al. have shown that in substituted tolans, at least two distinct electronically excited states can be detected in picosecond transient absorption, following excitation to the lowest energy absorption band. They also showed that the ordering (at least in the nonpolar solvent hexane) depends on the substituent. In *p*-aminodiphenylacetylene, the authors attributed a small ($<$1%) long (350 ps) component in emission to unimolecular barrier recrossing from the A_g (S_1) state to the allowed B_{1u} state. In cyano-diphenylacetylene, they assigned the lowest excited-state as B_{1u}. In compounds for which no evidence of additional low-lying electronic states were observed in transient absorption, the emission was characterized by a relatively weak temperature dependence and high quantum yield ($>$0.2). Two-photon-induced emission has not been observed in any of these molecules to date.

TABLE 2: Best-Fit Parameters for Nonradiative Rates

	H_{RP} (cm^{-1})	ΔG_P (cm^{-1})	$k_{nr}{}^a$ (s^{-1})
A	1.7	17900	6.5×10^8
B	8.6	17100	1.8×10^{10}
C	1.5	16800	5.1×10^8

[a] The maximum k_{nr} obtained from the fits.

We expect S_x in **A**−**C** (correlated to the B_{1u} state in **D**) to be the lowest excited singlet state in solution for the following reasons. The compound **A** is a cyano- and thiomethyl-substituted tolan. Its fluorescence quantum yield is high, and its radiative lifetime is relatively short ($\approx$3 ns). Unlike the case in **D**, measurements at reduced temperatures show that the emission lifetimes of **A** and **B** in hexane are only weakly dependent on temperature, with an apparent activation barrier $\simeq$ 0.5 kcal/mol. If this were the energy gap between S_x and S_1 in hexane, with S_x being of slightly higher energy than S_1, the large solvatochromic shift of S_x in even slightly polar solvents would reverse the ordering of energy levels.

Our estimate of k_{nr} from quantum yield and lifetime data assumes that the emissive state is the initially excited state and that nonradiative processes connect it to one or more nonemitting states. In principle, an alternative path in which the initial excited state is rapidly depopulated to the emissive state is also possible, as in the case where an LE $\rightarrow$ CT transition is involved. A mismatch between the radiative rate constant calculated from the oscillator strength of the absorption band and that calculated from the quantum yield and lifetime measurements could be considered evidence for rapid electronic state switching. In the case of **A** and **C**, absorption and emission measurements yield k_r values that are self-consistent. The corresponding values for **B** are significantly different—$k_r = (15\ \text{ns})^{-1}$ from emission results, as opposed to an estimated value of $(3\ \text{ns})^{-1}$ from the absorption oscillator strengths. As is apparent in Figure 3, there are several clearly discernible peaks in the absorption spectrum of **B**. We have measured essentially the same relative quantum yield for excitation at frequencies corresponding to the two lowest energy absorption peaks. Two peaks are distinctly seen in the emission spectrum of **B** in nonpolar solvents, suggesting that at least some of the features in the absorption spectrum are vibronic in character. However, it is possible that the presence of underlying electronic transitions to higher excited states in this region results in an overestimate of the oscillator strength of the lowest excited state. An analysis of a kinetic scheme explicitly considering overlapping absorption bands and nonradiative transitions between these electronic states (Appendix) shows that our estimates of k_{nr} are not likely to be significantly different from the values in Table 2. The smaller radiative rate constant of **B** may be the result of larger coupling with a triplet state.

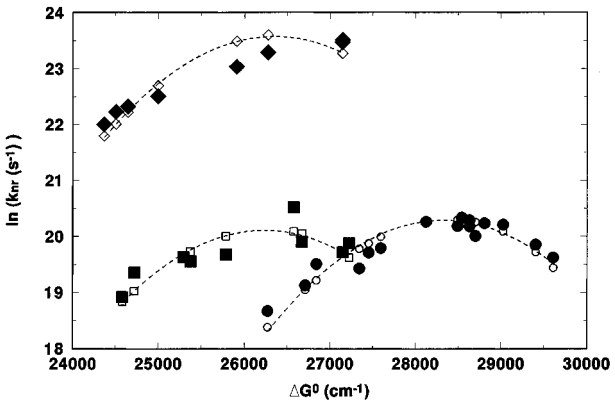

Figure 5. Nonradiative rate constants for **A**−**C** and best-fit lines. The filled symbols represent experimental data (●, **A**; ◆, **B**; ■, **C**) and the corresponding empty symbols represent best fit values obtained by nonlinear optimization. Data for **A** are from ref 10.

Charge Recombination and Classical ET Theory. The well-known classical expression for nonadiabatic electron transfer[33] is shown in

$$k_{et} = \frac{4\pi^2|H_{RP}|^2}{h\sqrt{4\pi\lambda kT}} \exp\left(-\frac{(\Delta G^\circ + \lambda)^2}{4\lambda kT}\right) \quad (1)$$

Here k_{et} is the rate constant and H_{RP} is the electronic matrix element for charge recombination. If, as previously,[10] we assume that the final state is similar to the ground state (hence nonpolar) but displaced on the free energy scale, the emission and absorption maxima in different solvents can be used to estimate the driving force (ΔG°) and the reorganization energy, λ:

$$-\Delta G^\circ = 0.5h(\nu_{abs} + \nu_{em}) - \Delta G_P \quad (2)$$

$$\lambda = 0.5h(\nu_{abs} - \nu_{em}) + \lambda_{in}$$

where ΔG_P is the difference in free energy between the "dark" state and S_0, λ_{in} is the intramolecular component of the total reorganization energy, and ν_{abs} and ν_{em} are the frequencies of the absorption and emission maxima, respectively. We assume that ΔG_P is independent of solvent or, equivalently, that the "dark" state is nonpolar. The electronic matrix element, H_{RP}, is then obtained from a nonlinear minimization of the sum of least-squares deviation using Newton's method, with ΔG_P and H_{RP} as independent variables. Nonlinear optimization of the sum of squared deviations was performed using the implementation of Newton's method in Quattro Pro V5.0. The value of λ_{in} was held constant at 1.0 eV, to get a reasonable match between the data and the fits, as smaller values resulted in narrower parabolas. Experimental data and best fit lines are shown in Figure 5. The optimum values (Table 2) show that H_{RP} is largest for **B**. Although a fit of k_{nr}, obtained in different solvents, to eq 1 is predicated on several assumptions, e.g., H_{RP} is solvent independent and that the intramolecular contribution to the reorganization can be treated classically, the relative size of H_{RP} should not be sensitive to these approximations. In a previous study on amino and nitro substituted tolans with varying number of acetylene spacers, Stiegman et al.[34] suggested that the decreasing quantum yield observed could be explained by invoking the Fermi Golden Rule, either as a consequence of a larger electronic coupling or as a result of the larger density of states available in the larger molecules. Our data indicate that it is the electronic coupling(s), and not the Franck−Condon weighted density of states which is responsible for the faster nonradiative decay in **B**.

The best-fit values of ΔG_P suggest that the "dark" state is fairly close in energy to the emitting triplet. The probes exhibit phosphorescence (77 K) about 18 000 cm^{-1}, which is only slightly higher than ΔG_P. In fluid solutions, we expect the energy of the triplet state will be somewhat lower due to dipolar stabilization. The difference could also be related to our ad hoc assumption of $\lambda_{in} = 1.0$ eV. However, it should be noted that a choice of smaller values resulted in fits of lower quality. This suggests that the lowest energy triplet state (T_1) is formed directly from the ^{1}CT, without the direct involvement of an intermediate state. Estimates based on semiempirical calculations[35] with limited configuration interaction (six electrons, five orbitals) yielded T_1 energies comparable to the measured phosphorescence energy, supporting this model. We presume that T_1 is not the ^{3}CT state on the basis of our model of the photophysics. The ^{3}CT state should have the same dipole moment as the ^{1}CT state and we would expect k_{nr} to be weakly solvent dependent. The calculations also show a second triplet state lower in energy than S_1. We have therefore included ^{3}CT in Figure 4 but do not consider it a dominant contributor to the observed dynamics.

Origin of Enhanced Electronic Coupling in B. The solvent dependence of k_{nr} implies that the nonradiative process is associated with a significant change in the electronic charge distribution, favoring an interpretation in terms of ET theory. The characteristic bell-shaped dependence of ET rates on driving force reflects the dynamics of nuclear reorganization associated with electron transfer. The overall magnitudes of the rate constants reflect the size of the perturbation or coupling. In systems where the donor and acceptor can be distinguished as separate chemical entities, the donor and acceptor are weakly coupled. The ET matrix element can be attributed to the Coulomb interaction between a donor electron and an acceptor. While these distinctions are best made in systems where the donor and acceptor are unlinked, diffusing species, they have also been applied successfully to linked systems where the interactions between the donor and acceptor are sufficiently weak for the two moieties to be considered spectroscopically distinct.[1,36] The absorption spectra (Figure 3) of the molecules being considered here indicate that the donor and acceptor states are fairly strongly coupled to the bridge. It is difficult to unambiguously identify a part of the molecule as the donor and another as the acceptor, although following our chemical intuition, we consider the thiomethyl and cyano groups as the donor and acceptor moieties, respectively. We performed semiempirical calculations[35] on **A**−**C** in an attempt to support our intuition. Results show the largest change in atomic charge upon excitation to be on the S atom ($\Delta e \approx +0.3$). The accompanying increase in electron density appears to be delocalized over the cyanophenyl part of the molecule. If we consider the S atom as the primary donor and the cyanophenyl group as the acceptor in **A**−**C**, the geometric distance for charge recombination increases from 10 Å in **A** to 13 Å in **B** and 17 Å in **C**. The change is even greater if "through-bond" distances are considered. Yet, H_{RP} for **C** is only slightly smaller than that for **A**; H_{RP} for **B** is *larger* than in the molecule with a shorter spacer, **A**. Clearly, H_{RP} does not follow a simple relation to molecular size. This is in contrast to the results found in donor−acceptor molecules with nonconjugated bridges, where an exponential decrease, i.e., $H_{RP} \approx H_0 \exp(-\beta(R - R_0))$ has been observed previously in several laboratories.[1]

The unusual dependence of H_{RP} in this series of molecules has several possible explanations. First, our estimates of the

distance parameter, *R*, are reliable only to the extent that the semiempirical calculations were correct in deducing the charge distribution in the lowest excited state of these molecules and that the calculated state is the one most appropriate for this study. If the observed trend in H_{RP} were merely a reflection of the inaccuracies in our estimates of *R*, we would have to conclude that charge delocalization involves the acetylene groups in **B** but not in **A** or **C**. To us, this would be quite surprising. Second, the existence of several low-lying electronic states increases the possibility of their participation in the recombination process by a superexchange mechanism. Third, as the absorption spectra show, the donor/acceptor levels are fairly strongly coupled to the bridge and the use of the exponential expression for the distance dependence of H_{RP} may be inappropriate. Fourth, if the "dark" state is a triplet and the exchange interaction is large, conservation of angular momentum will require significant spin−orbit (SO) interaction. The use of ET theory to explain our observations would not be strictly correct.

The similarity between the Marcus expression for the rate constant for nonadiabatic electron transfer and the expression for nonradiative decay in large polyatomic molecules has been noted previously.[37−39] This formal similarity reflects the fact that the exponential term arises from the nuclear reorganization required for the system to approach the crossing point. For a system in which the donor and acceptor are covalently linked, the difference between the two mechanisms can be difficult to establish. A rigorous description of the mechanism involves the determination of the individual coupling elements resulting from spin−orbit, coulomb, and spin-exchange interactions. In favorable cases, some of these interactions can be deduced from optical measurements carried out in the presence of a magnetic field. The relationship between H_{RP} (coupling resulting from coulomb interactions between the donor electron and the acceptor) and spin exchange has been described previously.[40]

In the preceding sections and the proposed kinetic scheme, we have indicated that the "dark" state is likely a triplet. The relevance of spin−orbit coupling to our results merits some discussion, specially considering that the symmetric molecules **E**−**G** also show phosphorescence at 77 K and nonradiative rate constants that are comparable to k_{nr} in the corresponding asymmetric molecules in nonpolar solvents. Coulomb exchange and spin−orbit coupling between states that are orbitally distinct, e.g., an $n\pi^*$ singlet (^{1}CT) coupled to a $\pi\pi^*$ triplet, would lead to a "concerted" charge recombination and intersystem crossing process. Stiegman et al.[34] had raised the possibility of smaller exchange interaction in molecules of increasing size, leading to enhanced intersystem crossing through hyperfine interactions (^{1}CT → ^{3}CT) as well as SO coupling. However, this would not explain the smaller apparent H_{RP} in the longer compound **C**.

The internal heavy atoms (S or N) in our molecules may contribute to SO coupling in these molecules.[15] The matrix element in *p,p′*-cyanomethoxydiphenylacetylene[12] is larger than the thiomethyl analogue, **A**, suggesting that the contribution of the nuclear charge of the S atom to intersystem crossing (ISC) is probably not important in these molecules. The π_x orbitals of the acetylene groups (i.e., those in the plane of the phenyl rings) may also contribute to ISC, a feature that was invoked to explain the rather large intersystem crossing rates in **D**.[30] A speculative interpretation of the H_{RP} values is that the π_x orbitals of adjacent acetylene groups interact strongly with each other and lead to enhanced coupling in **B**. When they are separated by a phenyl group, the acetylene groups behave as independent units. We are currently pursuing optical and ESR measurements to resolve the contribution of SO interactions to the observed electronic coupling in these systems.

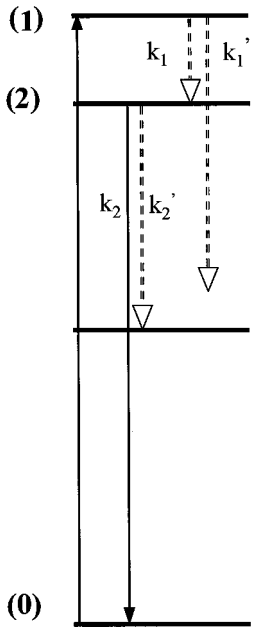

Figure 6. Kinetic scheme for the analysis of quantum yield and rate constants for two overlapping states in the absorption spectrum. Nonradiative processes are shown with shaded lines and arrow. Absorption and radiative processes are shown with dashed lines and open arrowheads. The rate constants k_1 and k_1' are the nonradiative rate constants depopulating the higher excited state (1). The state (2) is the emissive state, and (3) is most likely a triplet state. The arrow corresponding to the k_1' process is drawn only part way to the (3) state in order to indicate that it represents the combination of all nonradiative relaxation processes for (1) other than the internal conversion leading to population in state (2).

Conclusions

The solvent dependence of nonradiative rate constants in a series of acetylene-bridged molecules can be interpreted in terms of a rapid, photoinduced charge separation followed by a slower recombination process. Our measurements show that the electronic component of the interaction responsible for recombination is probe dependent but does not correlate simply with molecular size. Additional studies to further elucidate these issues are planned.[41]

Acknowledgment is made to the donors of The Petroleum Fund, administered by the American Chemical Society, for partial support of this research (PRF-24199-G6). We are indebted to A. E. Stiegman (Florida State) for his gift of **A**, to Terry Devlin and D. J. Jebaratnam (NU) for assistance with synthesis and HPLC, and to P. Vouros, J. E. Cunniff, and J. Carlson (NU) for mass-spectrometric characterization of **B**, **E** and **F**. L.R.K. would also like to thank David E. Budil (NU) for invaluable discussions. T.B.M. thanks NSERC (Canada) for funding and Johnson-Matthey Ltd. for a loan of Pd salts. P.N. also thanks NSERC for a postgraduate scholarship.

Appendix

To assess the impact of two electronic states absorbing in the 300 nm region on our estimates of k_{nr}, we explicitly analyze a kinetic scheme (Figure 6) that incorporates nonradiative transitions from the more energetic excited state (1) to other states as well as the lowest excited state (2). We assume that emission is seen only from (2), based on measured fluorescence spectra.

The estimated quantum yield, ϕ_{obs}, is related to the true quantum yield, $\phi^{(2)}_{true}$, through a combination of the extinction coefficients, $\epsilon^{(1)}$ and $\epsilon^{(2)}$, of the two electronic states at the excitation wavelength, λ, and the probability for a nonradiative transition from (1) to (2), $P^{1\rightarrow 2}$:

$$\phi_{obs} = \frac{[\epsilon^{(1)} \cdot P^{1\rightarrow 2} + \epsilon^{(2)}]\phi^{(2)}_{true}}{\epsilon^{(1)} + \epsilon^{(2)}}$$

The solution of the kinetic equations gives the time-dependent population, $C^{(2)}$, of state (2) as

$$C^{(2)}(t) = \frac{k_1 C^{(1)}(0)}{\Omega}\left[e^{-(k_1+k_1')t} - \left(1 - \frac{C^{(2)}(0)\cdot\Omega}{k_1 C^{(1)}(0)}\right)e^{-(k_2+k_2')t}\right]$$

where $\Omega = (k_2 + k_2') - (k_1 + k_1')$ and $P^{1\rightarrow 2}$ is given by $P^{(1\rightarrow 2)} = k_1/(k_1 + k_1')$.

We observe essentially monoexponential decays in polar solvents that have subpicosecond relaxation times in our data. Therefore, we assume that one of the two exponential components is too fast for us to measure, i.e., either $(k_1 + k_1')$ or $(k_2 + k_2')$ is greater than 10^{11} s^{-1}.

Case 1: $(k_2 + k_2') \gtrsim 10^{11}$ s^{-1}. Assuming that k_2, the radiative rate constant for state (2), is similar to the $\approx$(3 ns)$^{-1}$ value seen for **A** and **C**, k_2' is $\approx 10^{11}$ s^{-1}, thus implying that the coupling element H_{RP} is even larger than the estimate in Table 2.

Case 2: $(k_1 + k_1') \gtrsim 10^{11}$ s^{-1}. In this case, we make the approximation $(k_1 + k_1') \gg (k_2 + k_2')$. The time dependence of $C^{(2)}(t)$ simplifies to

$$C^{(2)}(t) = [P^{1\rightarrow 2}C^{(1)}(0) + C^{(2)}(0)]e^{-(k_2+k_2')t}$$

The observed decay time constant corresponds to the lifetime of the process we are interested in, i.e., depopulation of the lowest state (2). In principle, ϕ_{obs} could be less than $\phi^{(2)}_{true}$. A comparison of absorption and emission spectra in nonpolar solvents indicates that the two lowest energy peaks in the near −UV band are associated with state (2). The excitation spectrum shows the same features as the absorption spectrum, implying that the emission yield is not strongly dependent on excitation wavelength in the 280−350 nm region. This point is corroborated by direct measurement of quantum yield at a few selected excitation wavelengths. Consequently, either $\epsilon^{(1)} \ll \epsilon^{(2)}$ in the wavelength region of interest, or $P^{1\rightarrow 2} \approx 1$. Both possibilities imply that the observed quantum yield is not likely to be very different from the actual yield, i.e., $\phi_{obs} = \phi^{(2)}{}_{true}$. Therefore, we conclude that our measured coupling element is significantly larger for **B** than for either **A** or **C**.

References and Notes

(1) Wasielewski, M. R. *Chem. Rev. (Washington, D.C.)* **1992**, *92*, 435.
(2) *Photoinduced Electron Transfer*; Fox, M., Chinon, M., Eds.; Elsevier: Amsterdam, 1988.
(3) Beratan, D. N.; Betts, J. N.; Onuchic, J. N. *J. Phys. Chem.* **1992**, *96*, 2852.
(4) Murphy, C. J.; et al. *Science* **1993**, *262*, 1025.
(5) Priyadarshy, S.; Risser, S.; Beratan, D. N. *J. Phys. Chem.* **1996**, *100*, 17678.
(6) Nguyen, P.; et al. In *Applications of Organometallic Chemistry in the Preparation and Processing of Advanced Materials*; Harrad, J. F., Laine, R. M., Eds.; Kluwer Academic: The Netherlands, 1995; p 333.
(7) Tour, J. M. *Chem. Rev. (Washington, D.C.)* **1996**, *96*, 537.
(8) Strukelj, M.; Jordan, R. H.; Dodabalapur, A. *J. Am. Chem. Soc.* **1996**, *118*, 1213.
(9) Priyadarshy, S.; Therien, M. J.; Beratan, D. N. *J. Am. Chem. Soc.* **1996**, *118*, 1504.
(10) Khundkar, L. R.; Stiegman, A. E.; Perry, J. W. *J. Phys. Chem.* **1990**, *94*, 1224.
(11) Stiegman, A. E.; et al. *J. Am. Chem. Soc.* **1991**, *113*, 7658.
(12) Biswas, M. Ph.D. Thesis, Northeastern University, Boston, MA, 1996.
(13) Nguyen, P.; et al. *Inorg. Chim. Acta* **1994**, *220*, 289.
(14) Nguyen, P. Ph.D. Thesis, University of Waterloo, Canada, 1995.
(15) Lakowicz, J. *Principles of Fluorescence Spectroscopy*; Plenum: New York, 1987.
(16) Khundkar, L. R.; Bartlett, J. T.; Biswas, M. *J. Chem. Phys.* **1995**, *102*, 6456.
(17) The Marquardt−Levenberg algorithm for nonlinear least-squares was coded in Turbo Pascal on an AT class personal computers. A recursion relation for evenly spaced data points was used to convolute the instrument response function with the decays and appropriate derivatives.
(18) Grinvald, A.; Steinberg, F. I. *Anal. Biochem.* **1974**, *59*, 583.
(19) Freshly prepared samples typically showed decays that were single exponential within our resolution.
(20) Biswas, M.; Khundkar, L. R., manuscript in preparation.
(21) Beer, M. *J. Chem. Phys.* **1956**, *25*, 745.
(22) Strickler, S. J.; Berg, R. A. *J. Chem. Phys.* **1962**, *37*, 814.
(23) Murov, S. L.; Carmichael, I.; Hug, G. L. *Handbook of Photochemistry*; Marcel Dekker, Inc.: New York, 1993.
(24) Mataga, N.; Kubota, T. *Molecular Interactions and Electronic Spectra*; Marcel-Dekker, Inc.: New York, 1970.
(25) Okuyama, K.; et al. *J. Phys. Chem.* **1984**, *88*, 1711.
(26) Hirata, Y.; Okada, T.; Mataga, N. *J. Phys. Chem.* **1992**, *96*, 6559.
(27) Hirata, Y.; Okada, T.; Nomoto, T. *J. Phys. Chem.* **1993**, *97*, 9677.
(28) Rettig, W. *Angew. Chem., Int. Ed. Engl.* **1987**.
(29) Pcmodel-386, V4.0, Serena Sofware.
(30) Ferrante, C.; Kensy, U.; Dick, B. *J. Phys. Chem.* **1993**, *97*, 13457.
(31) Maroncelli, M. *J. Mol. Liq.* **1993**, *57*, 1.
(32) Gutmann, M.; et al. *J. Phys. Chem.* **1992**, *96*, 2433.
(33) Marcus, R. A.; Sutin, N. *Biochem. Biophys. Acta* **1985**, *811*, 265.
(34) Stiegman, A. E.; et al. *J. Am. Chem. Soc.* **1987**, *109*, 5884.
(35) Mopac 6.0, distributed by Serena Software, 1992.
(36) Bolton, J. R.; Connolly, J. S. *Photoinduced Electron Transfer*; Fox, M. A.; Chinon, M., Eds.; Elsevier: Holland, 1988.
(37) Meyer, T. J. *Prog. Inorg. Chem.* **1983**, *30*, 389.
(38) Casper, J. V.; et al. *Chem. Phys. Lett.* **1982**, *91*, 91.
(39) Englman, R.; Jortner, J. *Mol. Phys.* **1970**, *18*, 145.
(40) Bertrand, P. *Chem. Phys. Lett.* **1985**, *113*, 104.
(41) Nguyen, P.; Marder, T. B.; 1996. The second-order nonlinear optical properties of the donor−acceptor bis(phenylethynyl) benzenes will be reported elsewhere.